Geomech. Geophys. Geo-energ. Geo-resour. (2024) 10:24
https://doi.org/10.1007/s40948-024-00748-y

ORIGINAL ARTICLE

A permeability model for the fractal tree-like fracture network with self-affine surface roughness in shale gas reservoirs

Bowen Hu · J. G. Wang · Rui Sun · Zhiye Zhao

Received: 12 July 2022 / Accepted: 10 January 2024

Abstract The complex natural fracture network with self-affine rough surface and branching characteristics significantly impacts the gas transport in shale gas reservoirs. However, its effects on the permeability have not been studied so far. This study proposes an analytical permeability model for the fractal tree-like fracture network with self-affine surface roughness and branching characteristics. Firstly, the self-affine rough profiles of fracture surface are generated at different fractal dimensions by the Weierstrass–Mandelbrot function and a rough fractal tree-like fracture network is constructed with these surface profiles and branching characteristics. Then, an analytical permeability model is proposed to consider the effects of fracture surface roughness and tree-like branching characteristics on gas flow. This analytical model is verified by numerical simulations. Finally, the velocity distribution of the fracture network and the sensitivity of its structure parameters are analyzed. It is found that eddy flow is more easily formed on rougher fracture surfaces with larger fractal dimension when their fracture aperture is at millimeter scale. The eddy flow disappears when the fracture aperture is at micron scale. Bigger gas flow resistance and more energy loss are observed for smaller fracture aperture and rougher fracture surface. The gas velocity in rough fractures decreases by 60% at micron scale, but decreases by 50% at millimeter scale. Gas flow resistance also increases with the increase of branch angle, branch level and length ratio, but decreases with aperture ratio. As a result, permeability decreases with fractal dimension, branch angle, branch level and length ratio, but increases with aperture ratio.

Article highlights

1. An analytical permeability model is developed for rough fractal tree-like fracture network.
2. The mechanisms for energy loss and gas flow resistance in fractures vary with fracture surface roughness and aperture scale.
3. The impact of surface roughness on gas velocity is more significant at smaller aperture scale.
4. Eddy flow and backflow only occur near the rough surface of branching fractures at millimeter scale.

B. Hu · J. G. Wang
State Key Laboratory for Geomechanics and Deep Underground Engineering, China University of Mining and Technology, Xuzhou 221116, China

B. Hu · Z. Zhao
School of Civil and Environmental Engineering, Nanyang Technological University, Nanyang Avenue, Singapore 639798, Singapore

J. G. Wang (✉) · R. Sun
School of Mechanics and Civil Engineering, China University of Mining and Technology, Xuzhou 221116, China
e-mail: jgwang@cumt.edu.cn; nuswjg@yahoo.com

Published online: 24 January 2024

Keywords Self-affine roughness · Fractal tree-like fracture network · Analytical permeability · Shale gas reservoir

1 Introduction

The fractures are usually of multi-scale heterogeneity and thus affect the nonlinear flow of fluids in geological formations. Fractures are the main fluid flow channels in geological formations for nuclear waste disposal (Wu and Wang 2020), geothermal resource development (Xin et al. 2020; Ye and Wang 2020), oil and gas exploitation (Zheng et al. 2020; Sharifi et al. 2021), and CO_2 geological storage (Wang and Wang 2018). These fractures may naturally form fracture networks by the expansion and connection of microcracks, holes and joint fissures. Artificial stimulations such as hydraulic fracturing can help to form a fracture network in shale gas reservoirs (Dou et al. 2021). A fracture network has two features: rough surface of each fracture and fractal tree-like branching, as shown in Fig. 1. The surface morphology of natural fractures is always rough, with self-affine surfaces and non-uniform aperture. Natural micro-fractures are interconnected and can be simplified as a fractal tree-like fracture network. These two features heavily affect the gas transport ability or permeability of this fracture network through the fracture aperture, connectivity, fracture length and surface roughness (Wang and Cheng 2020; Zheng et al. 2022; Wan et al. 2023). However, an analytical permeability model for the gas flow in the fracture network with rough surfaces has not been available.

The gas flow rate is usually calculated by the classical cubic law for fractures with two smooth parallel surfaces (Snow 1969; Witherspoon et al. 1980; Akbarzadeh and Chalaturnyk 2014; Feng et al. 2020). Numerous laboratory tests observe that the classical cubic law produces obvious errors in the calculation of the flow rate in rough fractures (Ju et al. 2013; Tzelepis et al. 2015; Liu et al. 2016; Yin et al. 2017). Thus, the cubic law for smooth fractures is not applicable to the rough fracture structures.

The cubic law has been modified for the gas flow in rough fractures. Jin et al. (2017) developed a permeability model for single fracture whose rough fracture profile is generated by Weierstrass–Mandelbrot (W–M) function. They analyzed the impacts of surface roughness on gas transport by considering the surface tortuosity, surface roughness and hydraulic tortuosity of a rough fracture. Zeng et al. (2018) predicted the permeability of the microchannels with self-affine rough surfaces through shale gas flow simulations. They found that the influence of surface roughness on shale gas transport is greater in the transition flow region than in the slip flow region. Wang et al. (2018) established a modified cubic law to estimate the flow rate of single-phase fluid in a rough fracture. Their model has a simple form compared to the standard cubic law and can more accurately describe the fluid flow properties in rough fractures. Zhang et al. (2019) simulated the water flow in the rough fracture with several rough elements of rectangular or triangular bulges regularly arranged on the fracture surface. They found that these rough elements increase flow resistance and cause the separation and backflow of flow streamlines. Ju et al. (2019)

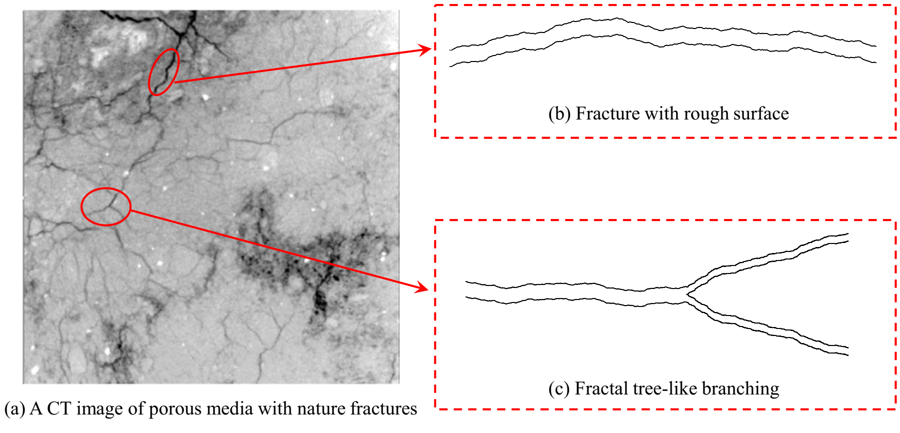

Fig. 1 The rough surface and fractal tree-like branching characteristic of nature fractures

proposed a water permeability model for rough fractures based on an optimized segmentation algorithm and self-affine rough profiles. Their self-affine rough profiles are generated by the W–M function and the optimized segmentation algorithm can decompose the fracture profiles into smaller parts. Dong and Ju (2020) further extended their optimized segmentation algorithm to the fractures with variable aperture and modified the cubic law. They used the lattice Boltzmann method (LBM) to simulate the water flow through the fracture with variable aperture (Guo et al. 2002). Liu et al. (2020a) proposed a successive random addition algorithm to generate a 3D rough surface of fractures and simulated the fluid flow through the 3D rough fractures. These previous studies only investigated the fluid flow in single rough fracture. The permeability and gas flow mechanisms within a rough fractal tree-like fracture network have not been investigated so far.

Fracture network has complex morphology and plays a key role in fluid flow mechanisms in shale oil or gas reservoir (Jafari and Babadagli 2012; Miao et al. 2015; Xu et al. 2016; Hu et al. 2019; Lahiri 2021). Jin et al. (2019) constructed several cleat networks in coal reservoirs based on self-affine rough fracture profiles and carried out the LBM simulation of gas flow in these cleat networks. They established an empirical formula to predict the permeability of cleat networks in coal reservoirs. Hu et al. (2020) generated several fractal discrete fracture networks in a shale gas reservoir based on the fractal distribution of fracture length. They simulated the shale gas transport in different fractal discrete fracture networks and observed that the cumulative production of shale gas is increased by 113% when fractal dimension increases from 1.5 to 1.7. Previous studies demonstrated that the distributions of fracture apertures and lengths follow fractal scaling laws, and corresponding permeability models for the fracture network have been developed based on fractal theory (Miao et al. 2015; Li et al. 2016; Wang et al. 2019; Gao et al. 2021). However, these previous permeability models assume that the fracture network is composed of a series of parallel fractures. This assumption simplifies the structure of fracture network but ignores the connectivity between fractures. This is derivated from the fact that the natural fracture networks in a shale gas reservoir are usually composed of intersected fractures. Therefore, the accurate description of the distribution of the intersected fractures is a challenge.

A complex fracture network can be described by the fractal tree-like fracture network model composed of a main fracture and several secondary branching fractures (Lorente et al. 2002; Xu and Yu 2006; Zheng and Yu 2012; Alalaimi et al. 2015; Zhang et al. 2021). When high pressure fluid is injected into a shale gas reservoir, hydraulic fractures interact with primary fractures to create more small fractures, thus increasing effective gas flow paths and enhancing shale gas production efficiency (Zhang et al. 2018; Dou et al. 2019). Xu et al. (2016) believed that the fractal tree-like fracture network can capture the statistical characteristics and topology of the fracture system in fractured porous media. They derived analytical expressions of effective permeability, tortuosity and fracture density for fractured porous media. Peng et al. (2019) proposed a thermal conductivity and an effective permeability model for a fractal tree-like fracture network and investigated the effects of structure parameters, such as length ratio, branch angle, branch level and width ratio on the heat transfer and fluid flow in the fracture network. Liu et al. (2020b) and Huang et al. (2020) developed their theoretical permeability models for the fractal tree-like fracture network with constant and variable aperture width. They found that the permeability of a fracture network with variable aperture is smaller than that of fracture network with constant aperture. These fractal tree-like fracture network models have been successfully applied to the complex fracture system of fractured porous media, but they are based on the smooth fracture surfaces in each branching and ignore the effect of surface roughness on the gas transport in complex fracture networks. The rough surfaces in each branching may have significant influences on the shale gas transport in a complex fracture network and should be further investigated.

In this study, an analytical permeability model is proposed for the rough fractal tree-like fracture network in fractured shale gas reservoirs. It considers the rough surface and branching characteristic of fracture network, which can effectively predict the permeability of fracture network of shale gas reservoirs, and is of great significance for unconventional oil and gas extraction. This paper is organized as follows. In Sect. 2, a rough fractal tree-like fracture network is constructed by self-affine rough surface profiles and branching characteristics, and an analytical permeability model is proposed to consider both surface roughness and branching characteristic of a rough fractal tree-like fracture network. In Sect. 3, the shale gas flow in the rough fractal tree-like fracture network is numerically simulated by the computational fluid dynamics (CFD) module within COMSOL software. In Sect. 4, the analytical permeability model is verified with the CFD simulations. In Sect. 5, the gas velocity distribution in the rough fractal tree-like fracture network at both micron and millimeter scales and the effects of structure parameters such as fractal dimension, length ratio, aperture ratio, branch level and branch angle on permeability are analyzed. Main conclusions are drawn in Sect. 6.

2 An analytical permeability model for a rough fractal tree-like fracture network

2.1 Construction of rough fractal tree-like fracture network

The fracture network is of great significance for the gas transport and permeability of shale gas reservoirs. Following Weierstrass–Mandelbrot (W–M) random function is used to characterize the rough fracture surface with self-affine property (Berry and Lewis 1980; Jin et al. 2017; Ju et al. 2017):

$$Z(x) = G^{D_f-1} \sum_{i=N_l}^{N_h} \gamma^{i(D_f-2)} \left[\cos(\phi_i) - \cos\left(\frac{2\pi\gamma^i x}{L_s} - \phi_i \right) \right] \tag{1}$$

where $Z(x)$ is the surface height at the coordinate x; D_f is the fractal dimension of fracture surfaces; γ is the rescaling factor that controls the density of the spectrum; G is the scaling constant; ϕ_i is the random number that ranges from 0 to 2π; L_s is the sample length; N_h and N_l control the maximum cosine frequency and minimum cosine frequency, respectively.

The rough fracture surface profiles with different fractal dimensions D_f are shown in Fig. 2. These profiles show that the fractal dimension D_f has a great influence on the morphology of fracture surfaces. A larger fractal dimension has a larger height range of surface profile and more obvious frequency variation. Figure 3 shows the diagrams of single rough fracture surface profile, a single rough fracture and a rough fractal tree-like fracture network. A single rough surface profile moves vertically for a short distance e_0, where e_0 can be regarded as the fracture aperture. A single rough fracture is formed by two rough surface profiles with the same shapes as shown in Fig. 3b. This single rough fracture is divided into two identical sub-branches according to the constant branching angle θ. A binary rough fracture architecture is shown in Fig. 3c. The length ratio α and aperture ratio β of the two adjacent branching levels are defined as

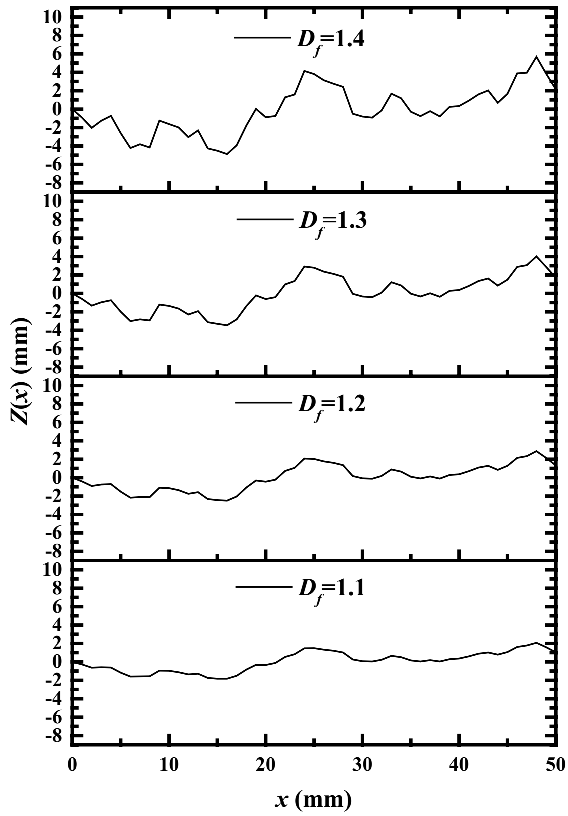

Fig. 2 Rough fracture surface profiles generated by the W-M function with different fractal dimensions

$$\alpha = \frac{l_{k+1}}{l_k} \tag{2}$$

$$\beta = \frac{e_{k+1}}{e_k} \tag{3}$$

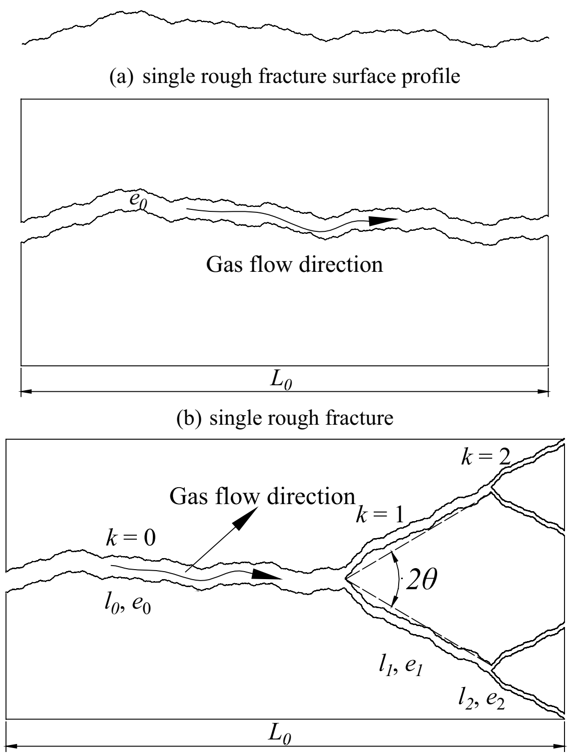

Fig. 3 Construction of a rough fractal tree-like fracture network

where l and e are the fracture length and aperture; the subscript k or $(k+1)$ denotes the fracture branching level. Thus, the fracture length and aperture at the kth level are

$$l_k = l_0 \alpha^k \tag{4}$$

$$e_k = e_0 \beta^k \tag{5}$$

2.2 A permeability model for single rough fracture

The gas flow rate q in a single fracture with two parallel flat plates is calculated by the classical cubic law:

$$q = \frac{we^3}{12\mu}\frac{\Delta P}{l} \tag{6}$$

where w is the fracture width; ΔP is the pressure difference between the inlet and the outlet; μ is the fluid viscosity.

The rough surface morphology in Fig. 2 has a great influence on shale gas flow. The roughness has three effects (Jin et al. 2017): the local roughness effect f_{local}, the surface tortuosity effect f_s, and the hydraulic tortuosity effect f_τ. Their total roughness effect f_{total} is then expressed by

$$f_{total} = f_{local} f_s f_\tau \tag{7}$$

The local roughness effect f_{local} is semi-empirically expressed as (Witherspoon et al. 1980)

$$f_{local} = 1 + \alpha_c \left(\frac{\sigma}{e}\right)^{\alpha_e} \tag{8}$$

where σ is the root mean square of surface height; α_c and α_e are the two fitting parameters related to the surface geometry.

The tortuous surface geometry narrows fracture aperture which is modified as $e_m = e/\tau_s$. Thus, the surface tortuosity effect f_s is (Turcotte 1997)

$$f_s = \frac{e_m^2}{e^2} = \frac{1}{\tau_s^2} \tag{9}$$

where $\tau_s = A_s/A_0$ is the surface tortuosity; A_s and A_0 are the total area of the rough surface and its corresponding projection area. The rough surface area is calculated through the fractal scaling law as (Sun and Koch 1998)

$$A_s = A_0^{D_s/2} e^{2-D_s} \tag{10}$$

where D_s is the fractal dimension of surface tortuosity.

Thus, the surface tortuosity τ_s is

$$\tau_s = \frac{A_0^{D_s/2} e^{2-D_s}}{A_0} = \frac{e^{2-D_s}}{A_0^{1-D_s/2}} = \left(\frac{e}{\sqrt{A_0}}\right)^{2-D_s} \tag{11}$$

The gas flow rate q is replaced with q/τ to consider the hydraulic tortuous effect. The hydraulic tortuosity τ of a rough fracture is (Duda et al. 2011)

$$\tau = \frac{U}{U_x} \tag{12}$$

where U is the average flow velocity in fractures and U_x is the component of the average flow velocity U in the x direction. The ratio of $U/U_x = (q/\tau)/q_x$ is satisfied in the single fracture. The hydraulic tortuosity effect f_τ is expressed as

$$f_\tau = \frac{q_x}{q} = \frac{1}{\tau^2} \tag{13}$$

The tortuous fracture length $l_t(e)$ is related to the fracture aperture e and the tortuosity fractal dimension D_τ as (Yu and Cheng 2002)

$$l_t(e) = l^{D_\tau} e^{1-D_\tau} \tag{14}$$

The hydraulic tortuosity τ is the ratio of tortuous length $l_t(e)$ to the straight length l (Cai and Yu 2011):

$$\tau = \frac{l_t(e)}{l} = \left(\frac{e}{l}\right)^{1-D_\tau} \tag{15}$$

For a rough fracture, the D_τ and D_s are approximately equal to D_f and $D_f + 1$, respectively (Mandelbrot 1983). In order to eliminate the limitation that the fractures are composed of the parallel and smooth plates as described in Eq. (6), the total roughness effect should include the local roughness effect, the surface tortuosity effect and hydraulic tortuosity effect. Thus, the gas flow rate in a single rough fracture is

$$q = \frac{we^3}{12\mu f_{total}}\frac{\Delta P}{l} = \frac{we^3}{12\mu f_{local}}\frac{1}{\tau^2\tau_s^2}\frac{\Delta P}{l} = \frac{we^3}{12\mu f_{local}}\left(\frac{e}{l}\right)^{4(D_f-1)}\frac{\Delta P}{l} \tag{16}$$

2.3 A permeability model for a rough fractal tree-like fracture network

Each fracture branch at any branching level of a fractal tree-like fracture network can be regarded as a single fracture. Based on Eq. (16), the gas flow rate q_k of each fracture branch at the k^{th} level is

$$q_k = \frac{we_k^3}{12\mu f_{local}}\left(\frac{e_k}{l_k}\right)^{4(D_f-1)}\frac{\Delta P_k}{l_k} \tag{17}$$

Then, the total flow rate Q at the kth level in all fracture branches is

$$Q = n^k q_k = \frac{we_0^{4D_f-1}}{12\mu f_{local} l_0^{4D_f-3}}\left(\frac{n\beta^{4D_f-1}}{\alpha^{4D_f-3}}\right)^k \Delta P_k \tag{18}$$

where ΔP_k is the pressure difference of the kth fracture branch.

The total pressure difference ΔP of a fractal tree-like network is the sum of all ΔP_k:

$$\Delta P = \sum_{k=0}^{m}\Delta P_k = \sum_{k=0}^{m}\frac{12\mu f_{local} l_0^{4D_f-3} Q}{we_0^{4D_f-1}}\left(\frac{\alpha^{4D_f-3}}{n\beta^{4D_f-1}}\right)^k = \frac{12\mu f_{local} l_0^{4D_f-3}}{we_0^{4D_f-1}}\frac{1-\left(\frac{\alpha^{4D_f-3}}{n\beta^{4D_f-1}}\right)^{m+1}}{1-\frac{\alpha^{4D_f-3}}{n\beta^{4D_f-1}}}Q \tag{19}$$

where m is the branch level.

This total gas flow rate Q is expressed by the Darcy's law as

$$Q = A\frac{K_F}{\mu}\frac{\Delta P}{L} = wE\frac{K_F}{\mu}\frac{\Delta P}{L} \tag{20}$$

where K_F is the permeability; $A = wE$ is the cross-sectional area of rough fractal tree-like network. The height E of the rough fractal tree-like network is

$$\begin{aligned} E &= e_0 + 2\left(l_1\sin\theta + l_2\sin\theta + \cdots + l_m\sin\theta\right) \\ &= e_0 + 2l_0\alpha\sin\theta\frac{1-\alpha^m}{1-\alpha} \\ &\approx 2l_0\alpha\sin\theta\frac{1-\alpha^m}{1-\alpha} \end{aligned} \tag{21}$$

The length L of the rough fractal tree-like network is

$$\begin{aligned} L &= l_0 + l_1\cos\theta + l_2\cos\theta + \cdots + l_m\cos\theta \\ &= l_0\left(1 + \alpha\cos\theta\frac{1-\alpha^m}{1-\alpha}\right) \end{aligned} \tag{22}$$

Substituting Eqs. (19), (21) and (22) into Eq. (20) obtains the permeability of the rough fractal tree-like network as

$$K_F = \frac{e_0^{4D_f-1}}{12 f_{local} l_0^{4D_f-3}}\frac{\left(1+\alpha\cos\theta\frac{1-\alpha^m}{1-\alpha}\right)}{2\alpha\sin\theta\frac{1-\alpha^m}{1-\alpha}}\frac{1-\frac{\alpha^{4D_f-3}}{n\beta^{4D_f-1}}}{1-\left(\frac{\alpha^{4D_f-3}}{n\beta^{4D_f-1}}\right)^{m+1}} \tag{23}$$

Equation (23) is our analytical permeability model for a rough fractal tree-like fracture network. When $f_{local} = 1$ and $D_f = 1$, which ignores the surface roughness, the permeability becomes

$$K_F = \frac{e_0^3}{12l_0}\frac{\left(1+\alpha\cos\theta\frac{1-\alpha^m}{1-\alpha}\right)}{2\alpha\sin\theta\frac{1-\alpha^m}{1-\alpha}}\frac{1-\frac{\alpha}{n\beta^3}}{1-\left(\frac{\alpha}{n\beta^3}\right)^{m+1}} \tag{24}$$

When $m = 0$, which ignores the branching characteristic, the permeability model of Eq. (23) is simplified into

$$K_F = \frac{e_0^{4D_f-1}}{12f_{local}l_0^{4D_f-3}} \tag{25}$$

This is the permeability of single rough fracture and has the same expression as that proposed by Jin et al. (2017).

3 Numerical simulation on gas flow in a rough fractal tree-like fracture network

The gas flow in fractures is usually described by the Navier–Stokes equation, which consists of the conservation laws of mass and momentum as (Navier 1827; Stokes 1845):

$$\frac{\partial\rho}{\partial t} + \nabla u = 0 \tag{26}$$

$$\rho\frac{\partial u}{\partial t} + \rho(u\cdot\nabla)u = -\nabla p + \mu\nabla\cdot\left(\nabla u + (\nabla u)^T\right) \tag{27}$$

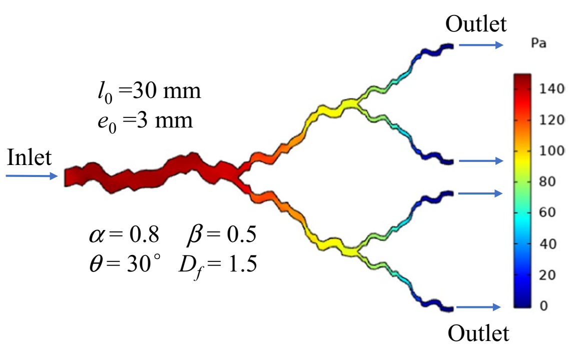

Fig. 4 Geometry of a rough fractal tree-like fracture network and gas pressure distribution

where u is the gas velocity; ρ is the gas density.

This Navier–Stokes equation is numerically solved by the computational fluid dynamics (CFD) module in COMSOL software. The geometrical structure of a rough fractal tree-like fracture network is shown in Fig. 4. For shale gas flow, the left boundary is the inlet and the right boundaries are the outlets. The pressure gradient is set between 1.4 and 12 kPa/m (Yin et al. 2020). The gas pressure of the inlet boundary is 120 Pa and the gas pressure of the outlet boundary is 0.01 Pa. The fracture surfaces are highly irregular, and the net movement of gas on their surfaces is almost negligible. Thus, the gas flow at the fracture surfaces can be regarded as no-slip boundary (Jin et al. 2017; Ju et al. 2019).

4 Model validation

4.1 Validation of simulation model

The experimental data of the single rough fracture from Yin et al. (2020) are used here to verify our simulation model. In their experiments, two single rough fractures with aperture of 1.0 mm and 1.5 mm are produced by the 3D printing technique. The fractures have the length of 100 mm and the fractal dimension of 1.2. In our simulation, the gas flow rate Q is obtained by integrating the flow velocity at the outlets. Figure 5 is the comparison of gas flow

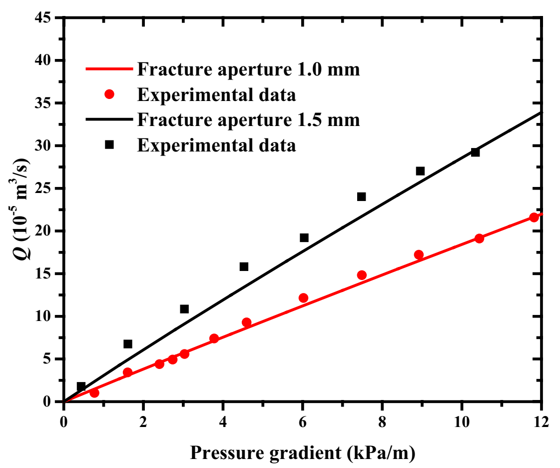

Fig. 5 Comparison of flow rate between experimental data and simulations

rate Q in the rough fracture between experimental data and simulation results. A clear linear relationship between gas flow rate and pressure gradient is observed when the fracture aperture is 1.0 mm. However, when the fracture aperture increases to 1.5 mm, they exhibit nonlinear characteristics, especially under high pressure gradient conditions. This may be because the gas flow rate increases with the increase of fracture aperture, resulting in a transition from linear to nonlinear gas flow. These simulation results match well with the experimental data of the two fractures. Hence, this simulation model can accurately describe the gas flow behavior in these rough fractures.

4.2 Validation of the analytical permeability model

The shale gas flow simulations in the rough fractal tree-like fracture network with $e_0 = 1 - 4$ mm are implemented to verify the analytical permeability model of Eq. (23) for the rough fractal tree-like fracture network. Other parameters are set as: $l_0 = 30$ mm, $D_f = 1.5$, $f_{local} = 1.05$, $\theta = 30°$, $\alpha = 0.8$, $\beta = 0.5$, m = 2, and n = 2. Figure 4 also shows the gas pressure distribution in the rough fractal tree-like fracture network and shale gas flows from the inlet to several outlets at the end of the last fracture branches. Further, the permeability can be calculated by the gas flow rate Q according to Eq. (20). The permeability is compared in Fig. 6 between numerical simulation and the analytical permeability model of Eq. (23). They are generally in agreement, although some deviations are observed. The derivations are small and within an acceptable range of error. Thus, this analytical permeability model can be used to predict the permeability of the rough fractal tree-like fracture network.

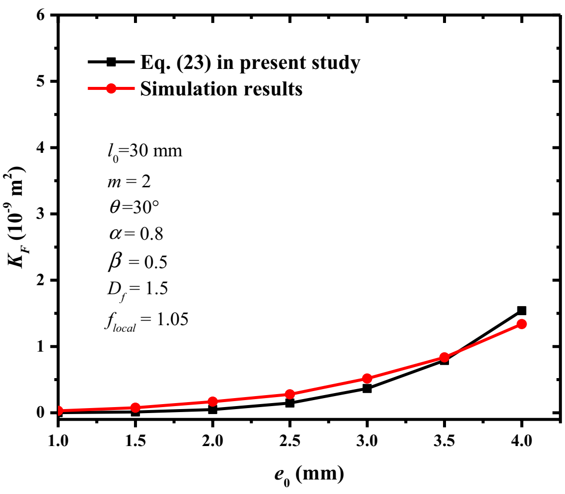

Fig. 6 Comparison of permeability between simulations and analytical model for the rough fractal tree-like network

5 Results and discussions

5.1 Velocity distribution

The fracture apertures are set at millimeter scale in some experiments and simulations of fluid flow within rough fractures (Ju et al. 2013, 2019; Yin et al. 2017), but SEM images observe that the apertures of most fractures in shale gas reservoirs are at micron scale (Yu et al. 2022). However, the gas flow simulation in the fractures at micron scale has not well investigated so far. This study carried out a series of gas flow simulations in the rough fractal tree-like fracture networks at millimeter scale and micron scale. The aperture e_0 of primary branch in the rough fractal tree-like fracture networks at millimeter scale is set as 1 mm, 2 mm, 3 mm and 4 mm, respectively, and length l_0 of primary branch is 30 mm. Correspondingly, the aperture e_0 of primary branch in the rough fractal tree-like fracture networks at micron scale is set as 1 μm, 2 μm, 3 μm and 4 μm, respectively, and length l_0 of primary branch is 30 μm. The fractal dimension of rough surface is set as 1.2, 1.3, 1.4 and 1.5, respectively.

The velocity distribution and streamlines in the fractal tree-like fracture network with smooth surface and rough surfaces are shown in Fig. 7 at millimeter scale and in Fig. 8 at micron scale. For the millimeter scale, Fig. 7 shows that the eddy flow occurs in the local rough areas where the channel height changes greatly. These local eddy flows increase the internal frictional resistance and produce a local energy loss. However, for the micron scale, no eddy flow occurs near the rough surfaces as shown in Fig. 8. This is because the gas flow velocity is very low in the fracture networks at micron scale and cannot generate the eddy flow. The rough surface hinders the shale gas transport in fractures and results in drastic changes in

Fig. 7 Streamlines at different fractal dimension in rough fractal tree-like network at millimeter scale

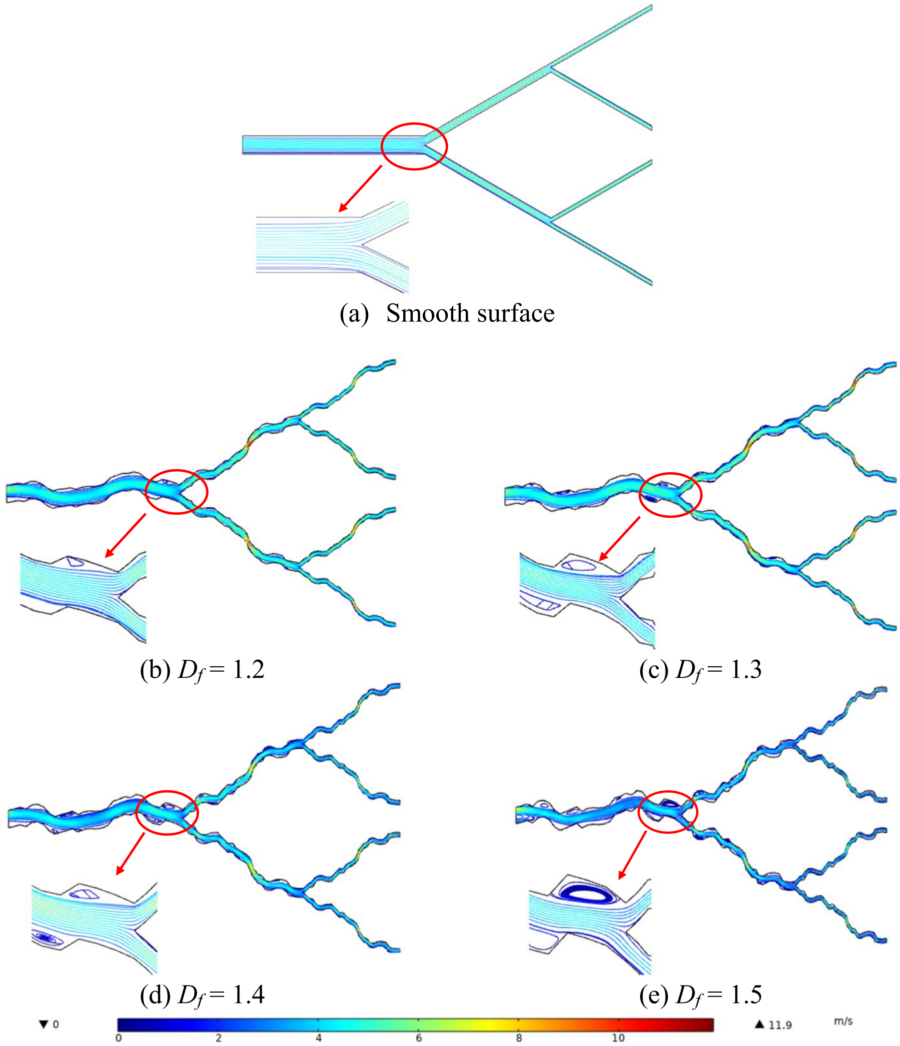

gas flow velocity in the narrow area of the fractures. The gas flow velocity is much larger at millimeter scale than at micron scale.

Figure 9a is the comparison of the average gas flow velocity of the outlets at millimeter scale when the fracture surface is smooth or rough. Generally, the gas flow velocity at outlets of fracture network with smooth surface is the highest and decreases with the increase of fractal dimension. If the smooth surface case is used as the base, the growth rate of gas flow velocity with different fractal dimensions is shown in Fig. 9b for the fracture network at millimeter scale. This gas flow velocity decreases by about 50% when $D_f = 1.5$. This phenomenon is mainly induced by two causes: One is that the rough surface increases the tortuosity of fractures and the streamline lengths of gas flow in fractures. The other is that the eddy flow more easily occurs near fracture surfaces for a higher fractal dimension. The increase of streamline lengths and eddy flow can increase the gas flow resistance and energy loss of shale gas, resulting in the decrease of gas flow velocity at the outlets. Similarly, the gas flow velocity and its growth rate at micron scale are presented in Fig. 10 for different fractal dimensions. Being different from millimeter scale, no eddy flow is observed near the rough surfaces at micron scale. The decrease of gas flow velocity at micron scale is only caused by the increase of gas flow path in fractures. As shown in Fig. 10b, the gas flow velocity at micron scale decreases by about 60% at $D_f = 1.5$, which is larger than that at millimeter scale. The

Fig. 8 Streamlines at different fractal dimension in rough fractal tree-like network at micron scale

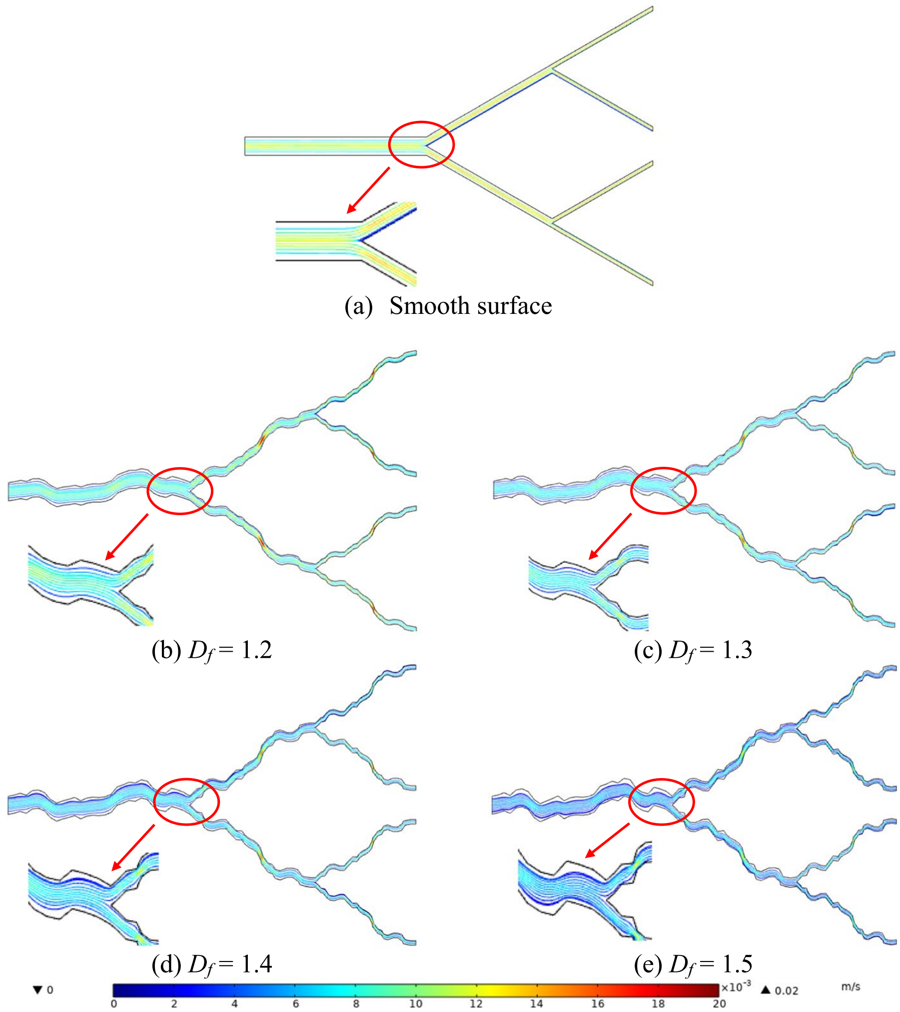

above analyses indicate that the reduction of gas flow velocity is more obvious for smaller fracture aperture and rougher fracture surface. This is because a smaller aperture will reduce the gas flow space, and a rougher surface will more easily hinder the gas flow in fractures. Thus, the gas flow resistance will be more significant for a fracture network with smaller aperture and rougher surface.

5.2 Impact of fractal dimension D_f on permeability

Fractal dimension D_f denotes the fracture surface roughness of a rough fractal tree-like fracture network. Figure 11 shows the effects of fractal dimension D_f on the permeability K_F of rough fractal tree-like fracture network under different e_0. It can be seen that the permeability K_F decreases with the increase of fractal dimension D_f. The increase of fractal dimension D_f means that the fractal tree-like fracture network has rougher surfaces. The local rough surface of fractures interferes with the gas flow and reduces the effective space for gas flow. Besides, higher fractal dimension of fractures also means higher tortuosity of fractures, which increases the length of shale gas flow path in fractures. The increase of gas flow length and the decrease of effective space increase the gas flow resistance, thus leading to the decrease of permeability of rough fractal tree-like fracture network.

5.3 Impacts of α and β on permeability

Length ratio α and aperture ratio β are two main scaling factors to structurally characterize the adjacent branches in a rough fractal tree-like fracture network.

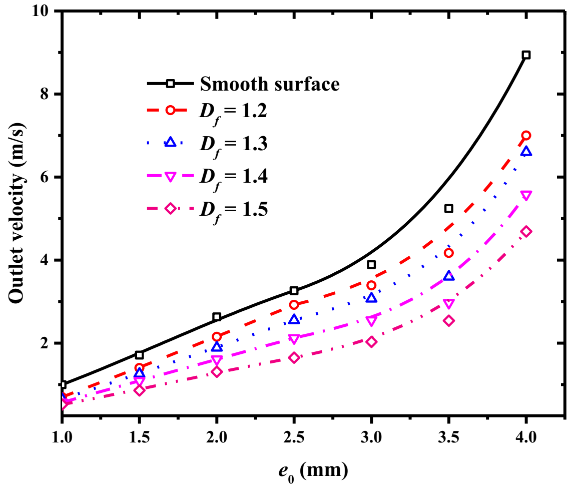

(a) Outlet velocity

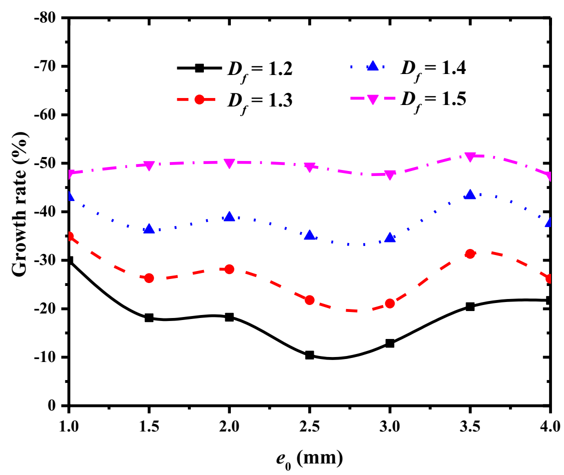

(b) Growth rate

Fig. 9 Variation of outlet velocity and its growth rate with fractal dimension at millimeter scale

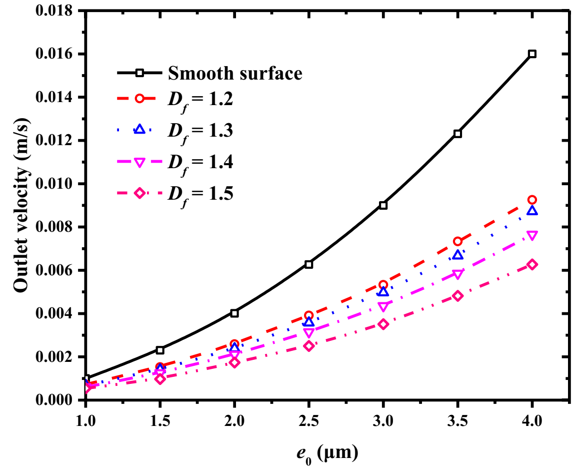

(a) Outlet velocity

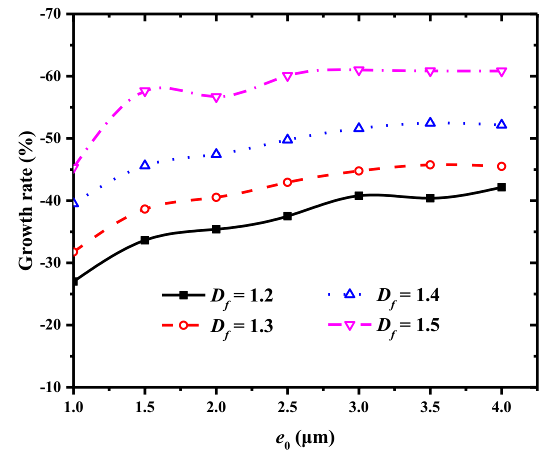

(b) Growth rate

Fig. 10 Variation of outlet velocity and its growth rate with fractal dimension at micron scale

Figure 12 shows the effects of length ratio α on the permeability K_F with different fractal dimension D_f. It is found that the permeability K_F logarithmically decreases with the increase of the length ratio α. Taking $D_f = 1.5$ as an example, the permeability of the rough fractal tree-like fracture network decreases from 3.83×10^{-17} to 1.96×10^{-20} m^2 when the length ratio α increases from 0.1 to 1.0. The reason is that the increase of length ratio α indicates an increase in the fracture length at the next branching levels and the total length L of rough fractal tree-like fracture network also increases. According to Eq. (22), the relationship between the total length L and length ratio α is shown in Fig. 13. The increase of length ratio α and the fracture length of the 0th level branch l_0 can increase the total length L of the rough fractal tree-like fracture network. Longer total length L means bigger gas flow resistance, thus the permeability of the rough fractal tree-like fracture network decreases.

The significant effect of aperture ratio β on permeability K_F is shown in Fig. 14. The permeability K_F increases with the increase of aperture ratio β under different fractal dimensions. When the aperture ratio β increases from 0.5 to 0.95, the permeability of the rough fractal tree-like fracture network with $D_f = 1.1$ increases from 2.24×10^{-15} m^2 to 2.73×10^{-14} m^2, and the permeability increases from

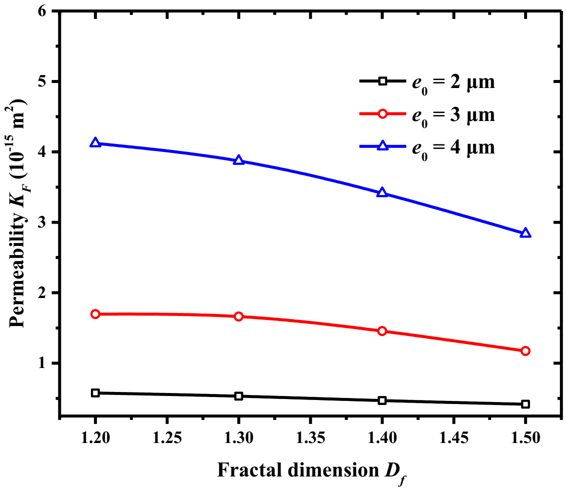

Fig. 11 Effects of fractal dimension D_f on the permeability K_F of the rough fractal tree-like fracture network

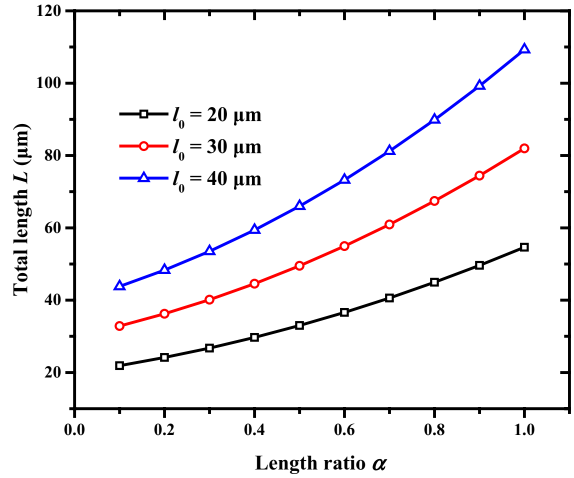

Fig. 13 Effects of the length ratio α on the total length L of the rough fractal tree-like fracture network

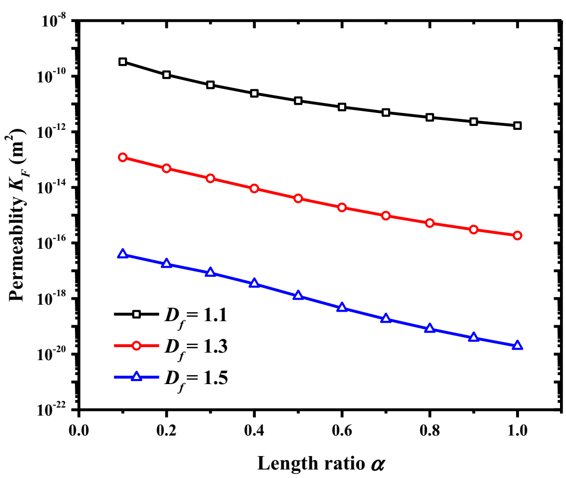

Fig. 12 Effects of length ratio α on the permeability K_F of the rough fractal tree-like fracture network

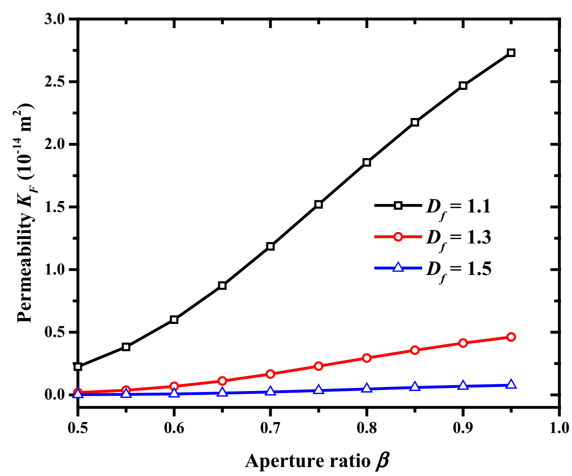

Fig. 14 Effects of the aperture ratio β on permeability K_F of the rough fractal tree-like fracture network

1.46×10^{-17} m^2 to 8.43×10^{-16} m^2 when D_f= 1.5. The permeability is much larger at D_f= 1.1 than at D_f= 1.5. This means that larger aperture ratio β and smoother fracture surfaces can provide larger gas flow spaces and lower gas flow resistance in sub-branching levels of the rough fractal tree-like fracture network. The effects of length ratio α and aperture ratio β on the permeability are consistent with the results from Liu et al. (2020b), but they ignore the rough surface of fracture branches in the fractal tree-like fracture network.

5.4 Impacts of m and θ on permeability

The distribution of branches in the rough fractal tree-like fracture network is determined by two structural parameters: branch level m and branch angle θ. Figure 15 shows the effects of the branch level m on permeability K_F at different fractal dimensions D_f. The logarithm of permeability K_F has an obvious negative linear relationship with the branch level m. When D_f= 1.5, the permeability K_F of the rough fractal tree-like fracture network decreases more

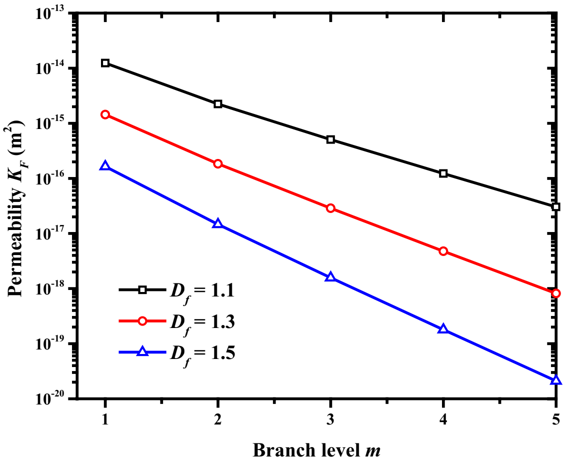

Fig. 15 Effects of the branch level m on permeability K_F of the rough fractal tree-like fracture network

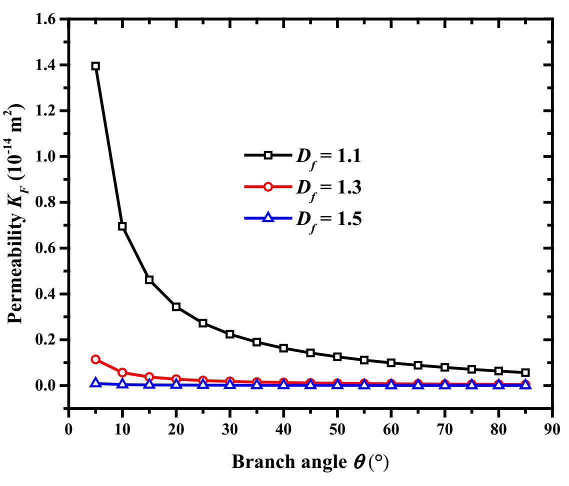

Fig. 16 Effects of the breach angle θ on permeability K_F of the rough fractal tree-like fracture network

significantly with the increase of branch level m than when $D_f = 1.1$. For $D_f = 1.5$, when the branch level m increases from 1 to 5, the permeability K_F decreases from 1.64×10^{-16} to 2.10×10^{-20} m^2 by more than 4 orders of magnitude. For $D_f = 1.1$, the permeability K_F decreases from 1.23×10^{-14} to 3.04×10^{-17} m^2, the permeability K_F decreases by approximately 3 orders of magnitude. It is because the increase of branch level m leads to the increase of the total number of smaller sub-branches. These smaller sub-branches reduce the permeability K_F. Figure 16 shows the impacts of branch angle θ on the permeability K_F with different fractal dimensions D_f. The permeability K_F decreases with the increase of branch angle θ. At $D_f = 1.1$, the permeability K_F decreases from 1.39×10^{-14} to 5.64×10^{-16} m^2 by approximately two orders of magnitude when the branch angle θ increases from 5° to 85°. This is because the energy loss at the branch node increases with the increase of branch angle θ. The variations of permeability with branch angle θ and branch level m are consistent with previous studies (Wang and Cheng 2020; Hu et al. 2021), but the surface roughness of each sub-branch is not considered in their models.

6 Conclusions

In this study, an analytical permeability model was proposed for a rough fractal tree-like fracture network in shale gas reservoirs. This fracture network was constructed by rough surface profiles and branching characteristics. Then, the analytical permeability model was verified with CFD simulations. Finally, the gas velocity distribution and the effects of structural parameters of rough fractal tree-like fracture network on permeability were analyzed. Based on these analyses, the main conclusions are drawn as follows:

Firstly, this analytical permeability model can well describe the branching characteristics and self-affine surface roughness of branch fractures in the fractal tree-like fracture network. It can be used to estimate the permeability of complex fracture network in shale gas reservoirs.

Secondly, the mechanisms for the energy loss and gas flow resistance in fractures vary with fracture surface roughness and aperture scale. At millimeter scale, the gas flow velocity in fractures is much larger than that at micron scale. Eddy flow and backflow are observed in the rough fractal tree-like fracture network at millimeter scale, while no eddy flow occurs at micron scale. Higher gas flow velocity is more likely disturbed by local rough surfaces.

Thirdly, the permeability K_F of rough fractal tree-like fracture network decreases with the increase of the branch level m, branch angle θ and length ratio α, but increases with the increases of aperture ratio β.

Larger aperture ratio β and smaller length ratio α will produce lower gas flow resistance and larger gas flow channel.

Acknowledgements The authors are grateful for the financial support from the National Natural Science Foundation of China (Grant No. 42030810, 51674246), the Postgraduate Research & Practice Innovation Program of Jiangsu Province (Grant No. KYCX21_2178), and the financial support from the China Scholarship Council (CSC, Grant No. 202006420048).

Declarations

Competing interests On behalf of all authors, the corresponding author states that there is no conflict of interest.

References

Akbarzadeh H, Chalaturnyk RJ (2014) Structural changes in coal at elevated temperature pertinent to underground coal gasification: a review. Int J Coal Geol 131:126–146

Alalaimi M, Lorente S, Wechsatol W, Bejan A (2015) The robustness of the permeability of constructal tree-shaped fissures. Int J Heat Mass Transf 90:259–265

Berry MV, Lewis ZV (1980) On the Weierstrass–Mandelbrot fractal function. Proc R Soc A 370(1743):459–484

Cai JC, Yu BM (2011) A discussion of the effect of tortuosity on the capillary imbibition in porous media. Transp Porous Media 89(2):251–263

Dong JB, Ju Y (2020) Quantitative characterization of single-phase flow through rough-walled fractures with variable apertures. Geomech Geophys Geo-Energy Geo-Resour 6:42

Dou FK, Wang JG, Leung CF, Ma ZG (2021) The alterations of critical pore water pressure and micro-cracking morphology with near-wellbore fractures in hydraulic fracturing of shale reservoirs. Eng Fract Mech 242:107481

Dou FK, Wang JG, Wang HM, Hu BW, Li CX (2019) Discrete element analysis for hydraulic fracture propagations in laminated reservoirs with complex initial joint properties. Geofluids, UNSP 3958583

Duda A, Koza Z, Matyka M (2011) Hydraulic tortuosity in arbitrary porous media flow. Phys Rev E 84(3):036319

Feng Q, Xu S, Xing X, Zhang W, Wang S (2020) Advances and challenges in shale oil development: a critical review. Adv Geo-Energy Res 4(4):406–418

Gao Q, Cheng YF, Han SC, Li Y, Yan CL, Han ZY (2021) Fractal analysis of shale gas transport through micropores and microfractures. Fractals 29(3):2150068

Guo ZL, Zheng C, Shi B (2002) Discrete lattice effects on the forcing term in the lattice Boltzmann method. Phys Rev E 65(4):046308

Hu BW, Wang JG, Li ZQ, Wang HM (2019) Evolution of fractal dimensions and gas transport models during the gas recovery process from a fractured shale reservoir. Fractals 27(8):1950129

Hu BW, Wang JG, Ma ZG (2020) A fractal discrete fracture network based model for gas production from fractured shale reservoirs. Energies 13:1857

Hu BW, Wang JG, Ma ZG, Sang SX (2021) Permeability and thermal conductivity models of shale matrix with a bundle of tortuous fractal tree-like branching micropore networks. Int J Therm Sci 164:106876

Huang N, Liu RC, Jiang YJ (2020) Evaluating the effect of aperture variation on the hydraulic properties of the three-dimensional fractal-like tree network model. Fractals 28(6):2050112

Jafari A, Babadagli T (2012) Equivalent fracture network permeability of multilayer-complex naturally fractured reservoirs. Transp Porous Media 91:339–362

Jin Y, Dong JB, Zhang XY, Li X, Wu Y (2017) Scale and size effects on fluid flow through self-affine rough fractures. Int J Heat Mass Transf 105:443–451

Jin Y, Zheng JL, Liu XH, Pan JN, Liu SX (2019) Control mechanisms of self-affine, rough cleat networks on flow dynamics in coal reservoir. Energy 189:116146

Ju Y, Zhang QG, Yang YM, Xie HP, Gao F, Wang HJ (2013) An experimental investigation on the mechanism of fluid flow through single rough fracture of rock. Sci China Technol Sci 56(8):2070–2080

Ju Y, Zhang QG, Zheng JT, Chang C, Xie HP (2017) Fractal model and lattice boltzmann method for characterization of non-Darcy flow in rough fractures. Sci Rep 7:41380

Ju Y, Dong JB, Gao F, Wang JG (2019) Evaluation of water permeability of rough fractures based on a self-affine fractal model and optimized segmentation algorithm. Adv Water Resour 129:99–111

Lahiri S (2021) Estimating effective permeability using connectivity and branch length distribution of fracture network. J Struct Geol 146:104314

Li B, Liu RC, Jiang YJ (2016) A multiple fractal model for estimating permeability of dual-porosity media. J Hydrol 540:659–669

Liu RC, Li B, Jiang YJ (2016) Critical hydraulic gradient for nonlinear flow through rock fracture networks: the roles of aperture, surface roughness, and number of intersections. Adv Water Resour 88:53–65

Liu RC, He M, Huang N, Jiang YJ, Yu LY (2020a) Three-dimensional double-rough-walled modeling of fluid flow through self-affine shear fractures. J Rock Mech Geotech Eng 12:41–49

Liu RC, Yu LY, Gao Y, He M, Jiang YJ (2020b) Analytical solutions for permeability of a three-dimensional fractal-like tree network model with fractures having variable widths. Fractals 28(1):2050013

Lorente S, Wechsatol W, Bejan A (2002) Tree-shaped flow structures designed by minimizing path lengths. Int J Heat Mass Transf 45:3299–3312

Mandelbrot BB (1983) The fractal geometry of nature. WH Freeman and Co., New York

Miao T, Yu B, Duan Y, Fang Q (2015) A fractal analysis of permeability for fractured rocks. Int J Heat Mass Transf 81:75–80

Navier C (1827) Mémoire sur les lois du mouvement des fluides. Mémoires De Académie Royale Des Sciences De Institut De France 6(2):389–440

Peng Y, Zhu XG, Cao B, Luo YQ, Zhou WJ (2019) Heat transfer and permeability of the tree-like branching networks. Int J Heat Mass Transf 129:801–811

Sharifi M, Kelkar M, Karkevandi-Talkhooncheh A (2021) A workflow for flow simulation in shale oil reservoirs: a case study in woodford shale. Adv Geo-Energy Res 5(4):365–375

Snow DT (1969) Anisotropic permeability of fractured media. Water Resour Res 5(6):1273–1289

Stokes G (1845) On the theories of internal friction of fluids in motion. Trans Camb Philol Soc 8(9):287–319

Sun HB, Koch M (1998) Fractal generation of surface area of porous media. Stoch Hydrol Hydraul 12:83–96

Turcotte DL (1997) Fractals and chaos in geology and geophysics. Cambridge University Press

Tzelepis V, Moutsopoulos KN, Papaspyros JNE, Tsihrintzis VA (2015) Experimental investigation of flow behavior in smooth and rough artificial fractures. J Hydrol 521:108–118

Wan XY, Cao JY, Yang X, Wang LF, Chen YC, Cheng BB (2023) Research on the flow field of the PEMFC bipolar plate based on the tree-like fractal theory. Fractals 31(8):2340185

Wang FY, Cheng H (2020) A fractal permeability model for 2D complex tortuous fractured porous media. J Petrol Sci Eng 188:106938

Wang HM, Wang JG (2018) Sealing efficiency analysis for shallow-layer caprocks in CO_2 geological storage. Environ Earth Sci 77:738

Wang ZH, Xu CS, Dowd P (2018) A modified cubic law for single-phase saturated laminar flow in rough rock fractures. Int J Rock Mech Min Sci 103:107–115

Wang JG, Hu BW, Wu D, Dou FK, Wang XL (2019) A multiscale fractal transport model with multilayer sorption and effective porosity effects. Transp Porous Media 129:25–51

Witherspoon PA, Wang JSY, Iwai K, Gale JE (1980) Validity of cubic law for fluid flow in a deformable rock fracture. Water Resour Res 16(6):1016–1024

Wu Q, Wang JG (2020) A thermo-hydro-mechanical coupling analysis for the contaminant transport in a bentonite barrier with variable saturation. Water 12:3114

Xin Y, Zhuang L, Sun ZX (2020) Numerical investigation on the effects of the fracture network pattern on the heat extraction capacity for dual horizontal wells in enhanced geothermal systems. Geomech Geophys Geo-Energy Geo-Resour 6:32

Xu P, Yu BM (2006) The scaling laws of transport properties for fractal-like tree networks. J Appl Phys 100:104906

Xu P, Li CH, Qiu SX, Sasmito AP (2016) A fractal network model for fractured porous media. Fractals 24(2):1650018

Ye ZW, Wang JG (2020) A coupling analysis for heat transfer and water flow in a fractal rough fracture of geothermal reservoirs. Fractals 28(6):2050100

Yin Q, Ma GW, Jing HW, Wang HD, Su HJ, Wang YC, Liu RC (2017) Hydraulic properties of 3D rough-walled fractures during shearing: an experimental study. J Hydrol 555:169–184

Yin PJ, Zhao C, Ma JJ, Yan CG, Huang LC (2020) Experimental study of non-linear fluid flow though rough fracture based on fractal theory and 3D printing technique. Int J Rock Mech Min Sci 129:104293

Yu BM, Cheng P (2002) A fractal permeability model for bi-dispersed porous media. Int J Heat Mass Transf 45(14):2983–2993

Yu HY, Lebedev M, Zhou JY, Lu MH, Li XL, Wang ZL, Han TC, Zhang YH, Johnson LM, Iglauer S (2022) The rock mechanical properties of lacustrine shales: argillaceous shales versus silty laminae shales. Mar Pet Geol 141:105707

Zeng Y, Ning ZF, Wang Q, Sun HL, Huang L, Ye HT (2018) Gas transport in self-affine rough microchannels of shale gas reservoir. J Petrol Sci Eng 167:716–728

Zhang XX, Wang JG, Gao F, Wang XL (2018) Numerical study of fracture network evolution during nitrogen fracturing processes in shale reservoirs. Energies 11:2503

Zhang Q, Luo SH, Ma HC, Wang X, Qian JZ (2019) Simulation on the water flow affected by the shape and density of roughness elements in a single rough fracture. J Hydrol 573:456–468

Zhang DC, Gao H, Dong QQ, Xiong CW (2021) Numerical study of forward and reverse flow characteristics of rough-walled tree-like fracture networks. Geomech Geophys Geo-Energy Geo-Resour 7:63

Zheng Q, Yu BM (2012) A fractal permeability model for gas flow through dual-porosity media. J Appl Phys 111:024316

Zheng JL, Jin Y, Liu XH, Wang C, Liu XK (2020) Validity of triple-effect model for fluid flow in mismatched, self-affine fractures. Adv Water Resour 140:103585

Zheng JL, Jin Y, Dong JB, Liu SX, Zhang Q, Song HB, Huang PH (2022) Reexamination of the permeability-aperture relationship for rough fractures with mismatched self-affine surfaces. J Hydrol 609:127727